NUCLEAR THEORY, Vol. 33 (2014)
eds. A.I. Georgieva, N. Minkov, Heron Press, Sofia

Microscopic Analysis of ^{10,11}Be Elastic Scattering on Protons and Nuclei

M.K. Gaidarov[1], **V.K. Lukyanov**[2], **D.N. Kadrev**[1], **E.V. Zemlyanaya**[2], **A.N. Antonov**[1], **K.V. Lukyanov**[2], **K. Spasova**[3,1]

[1]Institute for Nuclear Research and Nuclear Energy, Bulgarian Academy of Sciences, Sofia 1784, Bulgaria
[2]Joint Institute for Nuclear Research, Dubna 141980
[3]University "Ep. K. Preslavski", Shumen 9712, Bulgaria

Abstract. A microscopic approach to calculate the optical potential (OP) with the real part obtained by a folding procedure and with the imaginary part inherent in the high-energy approximation (HEA) is applied to study the ^{10,11}Be+p and ^{10,11}Be+^{12}C elastic scattering at energies of tens of MeV/nucleon, in addition to our previous studies of ^{6}He+p, ^{8}He+p, ^{6}He+^{12}C, and ^{11}Li+p scattering. The OPs and the cross sections are calculated using the Generator Coordinate Method (GCM) for the neutron and proton densities of ^{10,11}Be and the Quantum Monte Carlo (QMC) method for the latter of ^{10}Be. The depths of both components of the OP are determined from the comparison of the calculations with the available experimental data on the elastic scattering differential cross sections and taking into account the known behavior of the volume integrals as functions of the incident energy. The present approach, in which the only parameters are the depths of OPs, can be applied to calculations of more complex processes, such as diffraction breakup and stripping reactions.

1 Introduction

Proton elastic scattering is one of the simplest hadronic reactions and has been used to study various aspects of nuclei. Recently, the proton elastic scattering studies are applied for light neutron-rich nuclei. A major goal of the studies is to determine matter distributions, more specifically neutron distributions, in the neutron-rich nuclei and to argue existence of halo and/or skin structures.

Usually, it is accepted that the ^{11}Be nucleus consists of a core of ^{10}Be and a halo formed by a motion of a neutron in its periphery (e.g., Refs. [1–3]). The latter model is justified by the small separation energy $S_n = 504 \pm 6$ KeV [4] of a neutron from the ground $s_{1/2}$ state of ^{11}Be and on the observed quite large total interaction cross sections of ^{11}Be scattering on target nuclei with a main contribution from the breakup of ^{11}Be on ^{10}Be and a neutron. In addition, recent measurements of the charge radii of ^{7,9,10,11}Be revealed that the average distance between the halo neutrons and the dense core of the ^{11}Be nucleus is 7 fm [5] (see Figure 1). Thus, the halo neutron is about three times as far from the dense core

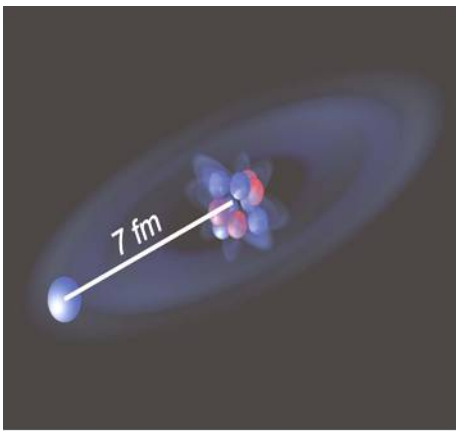

Figure 1. The "halo" nucleus ^{11}Be consists of a core of ^{10}Be and loosely bound neutron. Illustration: Dirk Tiedemann.

as is the outermost proton because the core itself has a radius of only 2.5 fm. The important role of a periphery is confirmed also by the experiments on scattering of ^{11}Be on the heavy nucleus of ^{208}Pb [6], where the prevailing mechanism is the direct breakup caused by the long-ranged Coulomb force of the nucleus. Also we should mention the important observation of the narrow peak in the momentum distribution of the ^{10}Be fragments at the breakup of ^{11}Be scattering on the ^{12}C nucleus [7], that is as mentioned above, a consequence of the large extension of the wave function of the relative motion in the (^{10}Be+n) system related to the small neutron separation energy.

The main aim of our work is to study the elastic scattering of the neutron-rich exotic ^{10}Be and ^{11}Be nuclei on protons and nuclei at energies $E < 100$ MeV/nucleon using microscopically calculated real and imaginary parts of the optical potentials. Very often the elastic scattering cross sections of ^{10,11}Be have been calculated using phenomenological OPs of given forms with numerous fitting parameters of their real and imaginary parts (e.g., Ref. [8]). Generally, much more advantages for such studies have the microscopical analyzes, such as that using the coordinate-space g-matrix folding method (e.g., Ref. [9]), as well as the work (e.g., Ref. [10]), where the real part of the OP (ReOP) is calculated microscopically using effective nucleon-nucleon (NN) interactions within a folding approach [11–14] and including also the exchange terms in it. In various works (e.g., Ref. [15]) the volume imaginary part of the OP (ImOP) has been taken phenomenologically either in a Woods-Saxon (WS) form or in the form of the direct folded ReOP.

In the present paper we continue our studies of the scattering of light exotic nuclei, such as ^{6}He [16, 17], ^{8}He [18], and ^{11}Li [19] using microscopic OPs within the hybrid model [20]. In the latter the ReOP is calculated by a folding

of a nuclear density and the effective NN potentials [13, 21]. The ImOP is obtained within the HEA [22,23]. There are only two or three fitting parameters in the hybrid model that are related to the depths of the ReOP, ImOP and the spin-orbit (SO) contribution to the OP. In the present work devoted to processes with ^{10,11}Be nuclei we use the density distribution for ^{10}Be obtained within the QMC [24] and also the densities of ^{10}Be and ^{11}Be obtained within the GCM [25].

2 Theoretical Scheme

In the present work we calculate the microscopic OP that contains a real part (V^F), an imaginary part (W) and the spin-orbit interaction (V^{LS} and W^{SO}). This OP is used for the calculations of the differential cross sections of the elastic scattering of the considered nuclei on protons or nuclear targets. We introduce a set of weighting coefficients N_R, N_I, N_R^{SO} and N_I^{SO} that are related to the depths of the corresponding components of the OP and are obtained by a fitting procedure to the available experimental data. Details of the constructing of the OP are given in Refs. [11–13, 21] (see also [16–19]). The OP has the form:

$$U(r) = N_R V^F(r) + iN_I W(r) - 2\lambda_\pi^2 \left[N_R^{SO} V_R^{SO} \frac{1}{r}\frac{df_R(r)}{dr} + iN_I^{SO} W_I^{SO} \frac{1}{r}\frac{df_I(r)}{dr} \right] (\mathbf{l}\cdot\mathbf{s}), \quad (1)$$

where $2\lambda_\pi^2 = 4$ fm^2. Let us denote the values of the ReOP and ImOP at $r = 0$ by $V_R(\equiv V^F(r=0))$ and $W_I(\equiv W(r=0))$. Then the parameters V_R^{SO} and W_I^{SO} in the spin-orbit part of the OP in Eq. (1) are related to V_R and W_I by the $V_R^{SO} = V_R/4$ and $W_I^{SO} = W_I/4$, correspondingly. We note that V_R and W_I (and V_R^{SO} and W_I^{SO}) have to be negative. The ReOP $V^F(r)$ is a sum of isoscalar (V_{IS}^F) and isovector (V_{IV}^F) components and each of them has its direct (V_{IS}^D and V_{IV}^D) and exchanged (V_{IS}^{EX} and V_{IV}^{EX}) parts.

The isoscalar component has the form:

$$V_{IS}^F(r) = V_{IS}^D(r) + V_{IS}^{EX}(r) = \int d^3\mathbf{r}_p d^3\mathbf{r}_t \{\rho_p(\mathbf{r}_p)\rho_t(\mathbf{r}_t) v_{NN}^D(\mathbf{s}) + \rho_p(\mathbf{r}_p, \mathbf{r}_p+\mathbf{s})\rho_t(\mathbf{r}_t, \mathbf{r}_t-\mathbf{s}) v_{NN}^{EX}(\mathbf{s}) \exp[i\mathbf{K}(r)\mathbf{s}/M]\}, \quad (2)$$

where $\mathbf{s} = \mathbf{r} + \mathbf{r}_t - \mathbf{r}_p$ is the vector between two nucleons, one of which belongs to the projectile and another one to the target nucleus.

In the first term of the right-hand side of Eq. (2) the densities of the incident particle ρ_p and the target nucleus ρ_t are sums of the proton and neutron densities. In the second term ρ_p and ρ_t are the corresponding one-body density matrices. In our work we use for them the approximations for the knock-on exchange term of the folded potential from Refs. [26, 27] (see also [16, 18]). In Eq. (2) $\mathbf{K}(r)$ is the local momentum of the nucleus-nucleus relative motion and v_{NN}^D and v_{NN}^{EX} are the direct and exchange effective NN potentials. They contain an

energy dependence usually taken in the form $g(E) = 1 - 0.003E$ and a density dependence in the form for the CDM3Y6 effective Paris potential [13]:

$$F(\rho) = C\left[1 + \alpha e^{-\beta\rho(\mathbf{r})} - \gamma\rho(\mathbf{r})\right] \tag{3}$$

with $C = 0.2658$, $\alpha = 3.8033$, $\beta = 1.4099$ fm^3, and $\gamma = 4.0$ fm^3. The effective NN interactions v^D_{NN} and v^{EX}_{NN} have their isoscalar and isovector components in the form of M3Y interaction obtained within g-matrix calculations using the Paris NN potential [12, 13] (see also [16]). The isovector components V^F_{IV} of the ReOP can be obtained by exchanging in Eq. (2) the sum of the proton and neutron densities in $\rho_{p(t)}$ by their difference and using the isovector parts of the effective NN interaction. In the case of the proton scattering on nuclei Eq. (2) contains only the density of the target nucleus.

The ImOP can be chosen either to be with the form of the microscopically calculated V^F ($W = V^F$) or in the form W^H obtained in Ref. [28] within the HEA of the scattering theory [22, 23]:

$$W^H(r) = -\frac{1}{2\pi^2}\frac{E}{k}\bar{\sigma}_N \int_0^\infty j_0(kr)\rho_p(q)\rho_t(q)f_N(q)q^2dq. \tag{4}$$

In Eq. (4) $\rho(q)$ are the corresponding formfactors of the nuclear densities, $f_N(q)$ is the amplitude of the NN scattering and $\bar{\sigma}_N$ is the averaged over the isospin of the nucleus total NN scattering cross section that depends on the energy. The parametrization of the latter dependence can be seen, e.g., in Ref. [16]. We note that to obtain the HEA OP (with its imaginary part W^H in Eq.(4)) one can have in mind the definition of the eikonal phase as an integral of the nucleon-nucleus potential over the trajectory of the straight-line propagation and has to compare it with the corresponding Glauber expression for the phase in the optical limit approximation. In the suggested scheme we use the known from other sources nuclear densities and NN cross sections and also the well known and already used NN potentials and amplitudes. In this way, the only free parameters in our approach are the depths (W's) of the OPs components. In the spin-orbit parts of the OP (the third term in the right-hand side of Eq. (1)) the functions $f_i(r)$ ($i = R, I$), according to the code DWUCK4 for solving the Schrödinger equation (that we use for the calculations of the cross sections) must correspond to WS forms of the potentials with parameters of the real and imaginary parts V_R, W_I, R_i, a_i [$f_R(r, R_R, a_R)$ and $f_I(r, R_I, a_I)$]. We determine the values of the parameters by fitting the WS potentials to the microscopically calculated potentials $V^F(r)$ and $W(r)$.

3 Results of Calculations and Discussion

In the calculations of the microscopic OPs for the scattering of ^{10,11}Be on protons and nuclei we used realistic density distributions of ^{10}Be calculated within

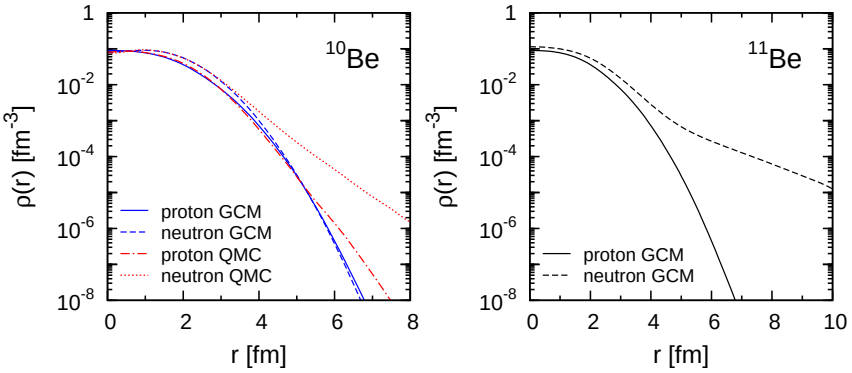

Figure 2. Point-proton (normalized to $Z = 4$) and point-neutron (normalized to $N = 6$ and $N = 7$, respectively) densities of ^{10}Be and ^{11}Be obtained in the GCM and in the QMC method.

the Quantum Monte Carlo Method [24] and of ^{10}Be and of ^{11}Be from the Generator Coordinate Method [25]. It can be seen from Figure 2 that they have been calculated with enough accuracy up to distances much larger than the nuclear radius. In both methods the densities of ^{10}Be are quite similar up to $r \sim 3.5$ fm and the difference between both of them can be seen in their asymptotics. In the calculations of the OPs for ^{10,11}Be+^{12}C the density was taken in symmetrized Fermy type [29].

On the basis of the scheme presented in Section 2 we calculated and compared with the data the elastic scattering cross sections of ^{10,11}Be+p at energies 38.4A MeV, 39.1A MeV [30] and 49.3A MeV and 59.4A MeV [8]. The results are given in Figures 3 and 4. Our analysis pointed out that more successful results are obtained in the case when the ImOP is taken from HEA: $W(r) = W^H(r)$ [Eq.(4)]. We note that in the fitting procedure of the theoretical results to the data for the elastic scattering cross sections for ^{10,11}Be+p (and also for ^{10,11}Be+^{12}C) there arises an ambiguity in the choice of the optimal curve among many of them that are close to the experimental data. Due to this we impose a physical constraint, namely to choose those ReOP and ImOP that give volume integrals which have a correct dependence on the energy. The volume integrals have the forms:

$$J_V(E) = -\frac{4\pi}{A_p A_t} \int drr^2 [N_R V^F(r)], \tag{5}$$

$$J_W(E) = -\frac{4\pi}{A_p A_t} \int drr^2 [N_I W(r)], \tag{6}$$

where A_p and A_t are the mass numbers of the projectile and the target, respectively.

It is known [31] that the volume integrals (their absolute values) for the

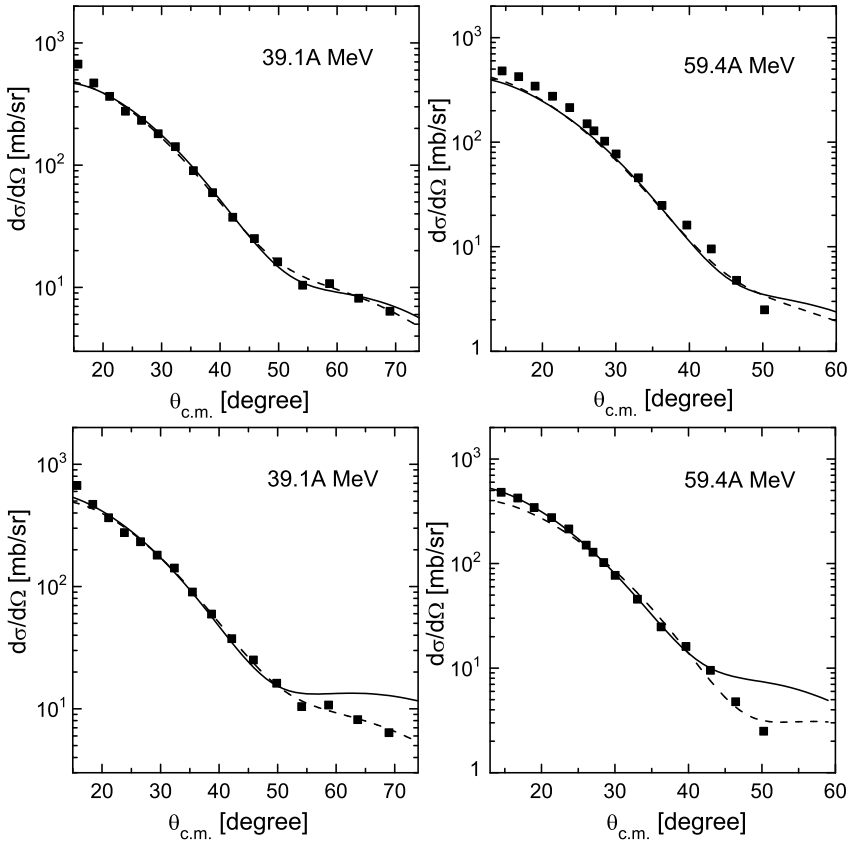

Figure 3. ^{10}Be+p elastic scattering cross sections. Upper panel: without SO term; bottom panel: with SO term. Solid lines: calculations with GCM density of ^{10}Be; dashed lines: calculations with QMC density of ^{10}Be. Experimental data for 39.1 MeV/nucleon and 59.4 MeV/nucleon are taken from Refs. [30] and [8], respectively.

ReOP have to decrease with the increase of the energy, while for the ImOP to increase. The values of the N's parameters from the fitting procedure and after imposing the mentioned constraint are given in Table 1. It can be seen from the Table that the tendency (the decrease of J_V and the increase of J_W) is generally confirmed. The comparison of the upper and the bottom panels of Figure 3 shows that the inclusion of the SO component of the OP gives a better agreement with the data of the calculations using the GCM density at energies 39.1A MeV and 59.4A MeV for angles less than 40° and 50°, correspondingly. There is a discrepancy at larger angles. At the same time for the cross sections with the account for the SO interaction and using the QMC density at energy 59.4A MeV there is only a small discrepancy with the data at small scattering angles.

Table 1. The renormalization parameters N_R, N_I, N_R^{SO} and N_I^{SO}, the total reaction cross sections σ_R (in mb), and the volume integrals J_V and J_W (in MeV.fm^3) as functions of the energy E (in MeV/nucleon) for the ^{10,11}Be+p elastic scattering

Nucleus	Model	E	N_R	N_I	N_R^{SO}	N_I^{SO}	σ_R	J_V	J_W
^{10}Be	GCM	39.1	0.983	0.267			292.12	389.408	116.600
without SO	QMC		1.153	0.295			311.36	411.344	130.806
interaction	GCM	59.4	1.001	0.802			341.18	333.739	263.540
	QMC		1.188	0.856			356.98	354.606	283.464
^{10}Be	GCM	39.1	1.493	0.492	1.000	0.476	372.50	591.440	216.480
with SO	QMC		1.163	0.318	0.557	0.000	323.96	414.911	141.004
interaction	GCM	59.4	1.294	0.804	0.190	0.000	355.29	431.427	264.197
	QMC		1.014	0.527	0.940	0.000	287.68	302.669	174.516
^{11}Be	GCM	38.4	0.824	0.659			459.05	339.388	293.493
		49.3	0.793	0.805			423.52	296.301	301.184

In general, the account for the spin-orbit term in the volume OP gives a trend of an increase of the cross sections at larger angles, that seems to be related with the change of the form of the total OP at its periphery. If we evaluate the quantities of the two densities of ^{10}Be on the basis of the values of the parameter N_R (comparing which ones are closer to unity), our conclusion is that in the calculations without SO interaction the GCM density works better, while in the case with SO term in OP the QMC density gives better results.

In Figure 4 are given and compared with the empirical data elastic cross

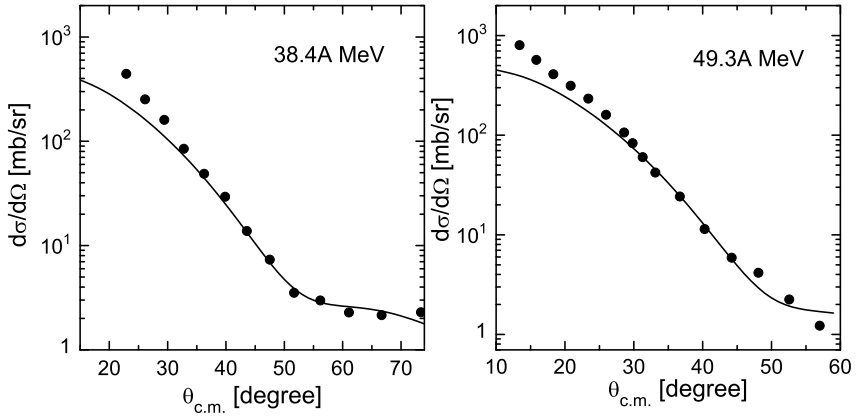

Figure 4. ^{11}Be+p elastic scattering cross sections. Calculations are performed with GCM density of ^{11}Be. Experimental data for 38.4 MeV/nucleon and 49.3 MeV/nucleon are taken from Refs. [30] and [8], respectively.

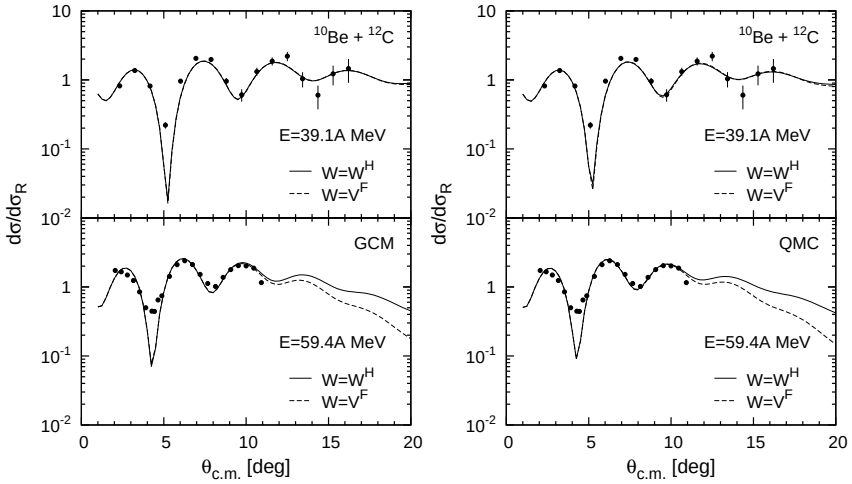

Figure 5. ^{10}Be+^{12}C elastic scattering cross sections. Solid lines: $W = W^H$; dashed lines: $W = V^F$. Left panel: calculations with GCM density of ^{10}Be; right panel: calculations with QMC density of ^{10}Be. Experimental data for 39.1 MeV/nucleon and 59.4 MeV/nucleon are taken from Refs. [30] and [8], respectively.

sections for the scattering of ^{11}Be on protons using the fitting procedure for the parameters N's. All of them are calculated using GCM density of ^{11}Be. One can see a discrepancy at small angles ($\theta < 30^\circ$) that seems to be related to the

Table 2. The renormalization parameters N_R and N_I, the total reaction cross sections σ_R (in mb), and the volume integrals J_V and J_W (in MeV.fm^3) as functions of the energy E (in MeV/nucleon) for the ^{10,11}Be+^{12}C elastic scattering

Nucleus	Model	E	W	N_R	N_I	σ_R	J_V	J_W
^{10}Be	GCM	39.1	W^H	0.939	0.708	104.539	255.156	283.037
			V^F	0.816	0.465	105.958	221.733	126.355
		59.4	W^H	1.013	1.010	101.052	238.122	302.581
			V^F	0.884	0.577	102.635	207.798	135.633
^{10}Be	QMC	39.1	W^H	0.888	0.620	105.332	245.613	249.769
			V^F	0.782	0.434	106.878	216.294	120.041
		59.4	W^H	0.970	0.887	101.616	231.953	267.782
			V^F	0.849	0.534	103.035	203.019	127.694
^{11}Be	GCM	38.4	W^H	0.769	0.711	127.123	216.879	287.235
			V^F	0.708	0.521	126.825	199.676	146.937
		49.3	W^H	0.820	0.883	124.406	213.754	300.193
			V^F	0.743	0.574	123.302	193.682	149.628

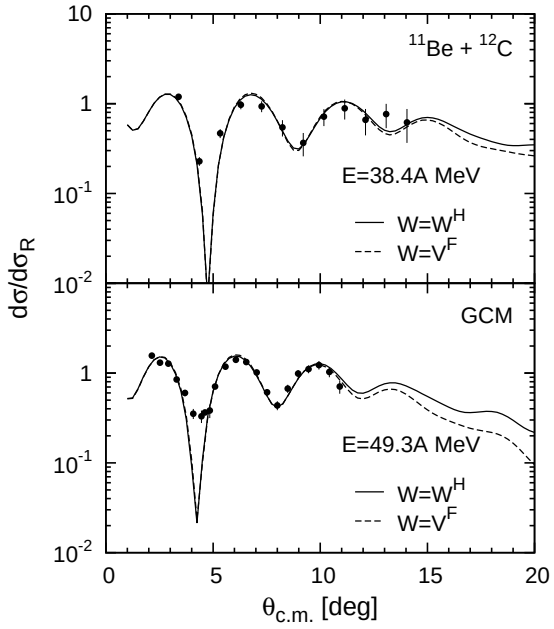

Figure 6. ^{11}Be+^{12}C elastic scattering cross sections. Solid lines: $W = W^H$; dashed lines: $W = V^F$. For ^{11}Be GCM density was used. Experimental data for 38.4 MeV/nucleon and 49.3 MeV/nucleon are taken from Refs. [30] and [8], respectively.

fact that in the calculations the coupling of the elastic channel with that when the weakly bound neutron is separated is not accounted for. In Table 1 are given the corresponding values of the parameters N_R and N_I whose values admit a deviation from unity of about 20–30$\%$ that pointed out the successful use of the hybrid model for OP in such calculations.

The calculated within the hybrid model elastic scattering cross sections of ^{10,11}Be+^{12}C (their ratios to the Rutherford one) are given in Figures 5 and 6 and compared with the experimental data. In comparison with the case of ^{10,11}Be+p, the experimental data [8, 30] for the scattering on ^{12}C demonstrate more developed diffractional picture on the basis of the stronger influence of the Coulomb field. It can be seen in Figure 5 that in both cases of the calculations of OPs with the QMC or GCM densities the results are in a good agreement with the available data. It is seen also from the figures that it is difficult to determine the advantage of the use for the ImOP, $W = W^H$ or $W = V^F$, because the differences between the theoretical results start at angles for which the experimental data are not available. The values of the parameters N_R and N_I (the depths of ReOP and ImOP) are given in Table 2. From the comparison of these values when GCM or QMC densities are used, one can see that in the case of GCM densities the values of the parameters are closer to unity. In this way, we may

conclude that as in the ^{10}Be+p case without SO term of OP, the GCM density can be considered as a more realistic one.

4 Conclusions

The hybrid model is applied to study characteristics of the processes of scattering of ^{10}Be and ^{11}Be on protons and nuclei. In the model the ReOP is calculated microscopically in a folding procedures of the densities of the projectile and the target with effective NN interactions related to the g-matrix obtained on the basis of the Paris NN potential. The ImOP is calculated microscopically within the high-energy approximation. The only free parameters in the hybrid model (N's) are the coefficients that correct the depths of the real, imaginary, and spin-orbit parts of the OP that are obtained by a fitting procedure to the experimental data whenever they exist. The density distribution of ^{10}Be obtained microscopically within GCM and QMC models and of ^{11}Be from GCM are used.

In this work, the elastic scattering cross sections of ^{10}Be and ^{11}Be on protons and ^{12}C are calculated using the microscopical OPs for energies $E < 100$ MeV/nucleon and are compared with the existing experimental data. In order to resolve the ambiguities of the magnitudes of the depths of the OPs the well established energy dependence of the respective volume integrals of the OP's is taken into account. The theoretical approach gives a good explanation of a wide range of empirical data on the ^{10,11}Be+p and ^{10,11}Be+^{12}C elastic scattering. It was established that the obtained by fitting procedure values of the coefficients N_R are close to unity. We conclude that, in general, the hybrid model for microscopical calculations of the OPs gives the basic important features of the scattering cross sections and can be recommended and applied to calculate more complex processes such as breakup reactions, momentum distributions of fragments and others.

Acknowledgements

The authors would like to thank the Russian Foundation for Basic Research (Projects Nos. 12-01-00396 and 13-01-00060), the Bulgarian Science Fund (Contract No. DID-02/16-17.12.2009), and Shumen University "Ep. K. Preslavski" (Contract No. RD-08-244/13.03.2014) for their support.

References

[1] M. Fukuda *et al.*, *Phys. Lett. B* **268** (1991) 339.
[2] N. Fukuda *et al.*, *Phys. Rev. C* **70** (2004) 054606.
[3] E. Gravo, R. Crespo, A.M. Moro, and A. Dentuva, *Phys. Rev. C* **81** (2010) 031601(R).
[4] H. Sagava, B.A. Brown, and H. Esbensen, *Phys. Lett. B* **309** (1993) 1.
[5] W. Nörtershäuser *et al.*, *Phys. Rev. Lett.* **102** (2009) 062503.
[6] T. Nakamura *et al.*, *Phys. Lett. B* **331** (1994) 296.

[7] J.H. Kelley *et al.*, *Phys. Rev. Lett.* **74** (1995) 30.

[8] M.D. Cortina-Gil *et al.*, *Phys. Lett. B* **401** (1997) 9; *Nucl. Phys. A* **616** (1997) 215c.

[9] K. Amos, W.A. Richter, S. Karataglidis, and B.A. Brown, *Phys. Rev. Lett.* **96** (2006) 032503; P.K. Deb, B.C. Clark, S. Hama, K. Amos, S. Karataglidis, and E.D. Cooper, *Phys. Rev. C* **72** (2005) 014608.

[10] M. Avrigeanu, G.S. Anagnostatos, A.N. Antonov, and J. Giapitzakis, *Phys. Rev. C* **62** (2000) 017001; M. Avrigeanu, G.S. Anagnostatos, A.N. Antonov, and V. Avrigeanu, *Int. J. Mod. Phys. E* **11** (2002) 249; M. Avrigeanu, A.N. Antonov, H. Lenske, and I. Stetcu, *Nucl. Phys. A* **693** (2001) 616.

[11] G.R. Satchler and W.G. Love, *Phys. Rep.* **55** (1979) 183; G.R. Satchler, *Direct Nuclear Reactions* (Clarendon, Oxford, 1983).

[12] D.T. Khoa and W. von Oertzen, *Phys. Lett. B* **304** (1993) 8; **342** (1995) 6; D.T. Khoa, W. von Oertzen, and H.G. Bohlen, *Phys. Rev. C* **49** (1994) 1652; D.T. Khoa, W. von Oertzen, and A.A. Ogloblin, *Nucl. Phys. A* **602** (1996) 98; D.T. Khoa and H.S. Than, *Phys. Rev. C* **71** (2005) 014601; O.M. Knyaz'kov, *Sov. J. Part. Nucl.* **17** (1986) 137.

[13] D.T. Khoa and G.R. Satchler, *Nucl. Phys. A* **668** (2000) 3.

[14] D.T. Khoa, G.R. Satchler, and W. von Oertzen, *Phys. Rev. C* **56** (1997) 954.

[15] M.Y.M. Hassan, M.Y.H. Farag, E.H. Esmael, and H.M. Maridi, *Phys. Rev. C* **79** (2009) 014612.

[16] K.V. Lukyanov, V.K. Lukyanov, E.V. Zemlyanaya, A.N. Antonov, and M.K. Gaidarov, *Eur. Phys. J. A* **33** (2007) 389.

[17] V.K. Lukyanov, D.N. Kadrev, E.V. Zemlyanaya, A.N. Antonov, K.V. Lukyanov, and M.K. Gaidarov, *Phys. Rev. C* **82** (2010) 024604.

[18] V.K. Lukyanov, E.V. Zemlyanaya, K.V. Lukyanov, D.N. Kadrev, A.N. Antonov, M.K. Gaidarov, and S.E. Massen, *Phys. Rev. C* **80** (2009) 024609.

[19] V.K. Lukyanov, D.N. Kadrev, E.V. Zemlyanaya, A.N. Antonov, K.V. Lukyanov, M.K. Gaidarov, and K. Spasova, *Phys. Rev. C* **88** (2013) 034612.

[20] K.V. Lukyanov, E.V. Zemlyanaya, and V.K. Lukyanov, *Phys. At. Nucl.* **69** (2006) 240; JINR Preprint P4-2004-115, Dubna, 2004.

[21] K.V. Lukyanov, JINR Comm. R11-2007-38, Dubna, 2007.

[22] R.J. Glauber, *Lectures in Theoretical Physics* (New York, Interscience, 1959), p.315.

[23] A.G. Sitenko, *Ukr. Fiz. J.* **4** (1959) 152.

[24] S.C. Pieper, K. Varga, and R.B. Wiringa, *Phys. Rev. C* **66** (2002) 044310.

[25] P. Descouvemont, *Nucl. Phys. A* **615** (1997) 261.

[26] X. Campy and A. Bonyssy, *Phys. Lett. B* **73** (1978) 263.

[27] J.W. Negele and D. Vautherin, *Phys. Rev. C* **5** (1972) 1472.

[28] K.V. Lukyanov, E.V. Zemlyanaya, and V.K. Lukyanov, *Phys. At. Nucl.* **69** (2006) 240; JINR Preprint P4-2004-115, Dubna, 2004.

[29] V.V. Burov and V.K. Lukyanov, Preprint JINR, R4-11098, Dubna, 2007; V.V. Burov, D.N. Kadrev, V.K. Lukyanov, and Yu. S. Pol', *Phys. At. Nucl.* **61** (1998) 525.

[30] V. Lapoux *et al.*, *Phys. Lett. B* **658** (2008) 198.

[31] E.A. Romanovsky *et al.*, *Bull. Russ. Acad. Sci.: Phys.* **62** (1998) 150.